# Dynamics of Muscle Microcirculatory Oxygen Exchange

DAVID C. POOLE, BRAD J. BEHNKE, and DANIELLE J. PADILLA

*Departments of Kinesiology, Anatomy and Physiology, Kansas State University, Manhattan, KS*

**ABSTRACT**

POOLE, D. C., B. J. BEHNKE, and D. J. PADILLA. Dynamics of Muscle Microcirculatory Oxygen Exchange. *Med. Sci. Sports Exerc.*, Vol. 37, No. 9, pp. 1559–1566, 2005. **Purpose:** Beyond the initial cardiodynamic "Phase I," pulmonary oxygen uptake ($\dot{V}O_2$) kinetics are dictated largely by, and resemble closely, the $\dot{V}O_2$ of the exercising muscles ($\dot{V}O_2m$). Within those muscles, the microcirculation is responsible for affecting almost all blood–myocyte $O_2$ transfer, and thus, observations at this site may provide key insights into muscle oxidative function in health and dysfunction in disease. **Methods:** Recently, a novel combination of microscopy and phosphorescence quenching techniques has been utilized to understand the dynamics of microvascular $O_2$ delivery ($\dot{Q}O_2m$) and muscle $O_2$ utilization ($\dot{V}O_2m$) at the onset of muscle contractions. **Results:** These experiments have addressed longstanding questions regarding the site of control of $\dot{V}O_2m$ kinetics and provide a first look at capillary hemodynamics at exercise onset in healthy muscle and their derangements resulting from chronic diseases such as heart failure and diabetes. **Conclusion:** This paper will review these novel findings within our current understanding of microcirculatory control and blood–myocyte $O_2$ transfer. **Key Words:** INTRAVITAL MICROSCOPY, PHOSPHORESCENCE QUENCHING, OXYGEN UPTAKE, CAPILLARY HEMODYNAMICS

## MYTHS AND THE MICROCIRCULATION

Before exploring recent findings, it is instructive to address some of the mythical dogmas, still prevalent in the literature, that obscure the understanding of structure-function relationships in the microcirculation.

**Capillary geometry.** Following the pioneering work of August Krogh in the early 20th century (26), it became convenient to consider capillaries as straight unbranched structures. However, examination of skeletal muscle microvascular corrosion casts by Ishikawa and colleagues ((16); see also (10)) and the elegant morphometric analyses of Mathieu-Costello, Weibel, and others (29) has revealed that capillaries display a complex three-dimensional geometry that is dependent principally upon muscle sarcomere length (Fig. 1, upper panel). Specifically, capillaries exhibit intercapillary connectivity (i.e., anastomoses) and a highly tortuous geometry at short physiological sarcomere lengths. As sarcomere length becomes greater, capillaries become straightened and stretched such that the narrowed lumens may impede red blood cell (RBC) flow (23,35).

**Capillary recruitment during exercise.** The opinion that many capillaries do not flow in resting muscle and are "recruited" during contractions, if true, would help explain the increased muscle $O_2$ diffusing capacity with exercise. However, there is solid experimental evidence in intact conscious animals (19) and multiple individual muscles examined by intravital microscopy (21–24,34) that the vast majority of capillaries support red blood cell (RBC) flux (i.e., flow) at rest. This raises the probability that the bulk of the increased capillary diffusing capacity in exercising muscle comes from combination of: A) a better utilization of capillary surface area along the length of individual capillaries, in part due to exercise-induced elevation of "tube" hematocrit (Hct) (and thus RBC-to-capillary surface contact) and also increasing the proximal-to-distal capillary length over which $O_2$ is exchanged; and B) intramyocyte effects related to the improved $O_2$ transport ability of deoxygenated versus oxygenated myoglobin (15).

**Capillary Hct.** The Hct within the capillary is certainly not the same as that found systemically. Rather, mean capillary Hct in resting muscle may be as low as 10–15% and becomes elevated towards systemic values (40–50%) during physiological or chemically induced hyperemia (8,22,24,25,43,44). Moreover, there is an enormous heterogeneity in Hct among capillaries with values ranging from 1 to 50% within the same muscle (22,44).

**$O_2$ partial pressure ($PO_2$) profile within muscle.** The notion that $PO_2$ during exercise falls systematically with increasing distance from the RBC to the mitochondria is contradicted by the finding of a low (1–4 mm Hg) and fairly uniform intramyocyte $PO_2$ ($PO_2intra$, (15,32,38)). Thus, $PO_2$ falls precipitously in that short physical space (0.5–2 $\mu$m) from the RBC (where it may approach arterial values >90 mm Hg) to the immediately subsarcolemmal cytoplasmic space (Fig. 1, lower panel and Fig. 2). Two of the most striking consequences of this behavior are: A) the greatest resistance to tissue $O_2$ diffusion is found in close proximity to the RBC, which means that events within the capillary are a primary determinant of muscle $O_2$ diffusing capacity (supported by the modeling studies of Groebe and

Address for correspondence: David C. Poole, Department of Anatomy and Physiology, Kansas State University, Manhattan, KS; E-mail: poole@vet.ksu.edu.
Submitted for publication December 2004.
Accepted for publication March 2005.

0195-9131/05/3709-1559/0
MEDICINE & SCIENCE IN SPORTS & EXERCISE®

DOI: 10.1249/01.mss.0000177471.65789.ce

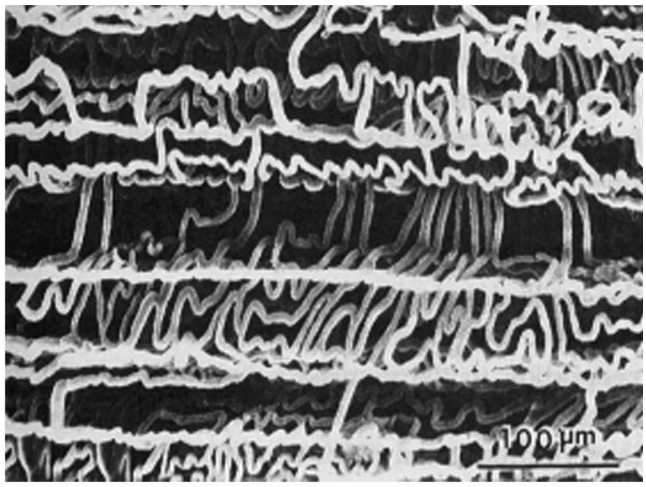


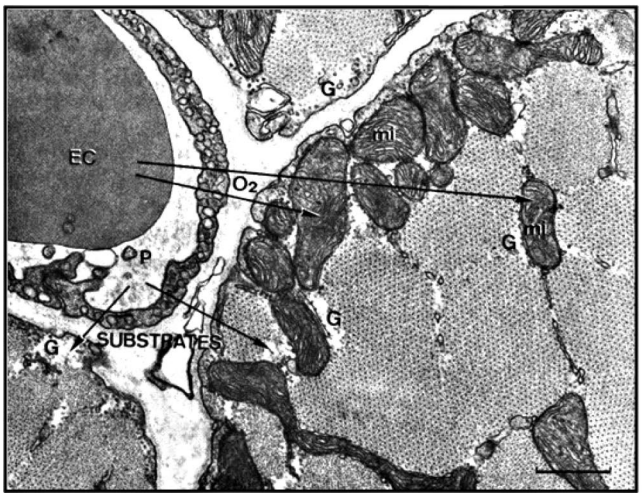


**FIGURE 1—*Top panel*: Corrosion cast (muscle fibers have been corroded away) of mouse soleus muscle showing geometry of the capillary bed (from Ishikawa and colleagues (16), used with permission). Skeletal muscle capillary beds possess a convoluted three-dimensional geometry with extensive intercapillary branching and become extremely tortuous at short muscle sarcomere lengths. *Bottom panel*: Electron micrograph showing the passage of $O_2$ from the RBC (erythrocyte, EC) to the mitochondria (mi). P, plasma; G, glycogen granules; bar, 0.5 µm. Note the extremely short physical space between the RBC and the subsarcolemmal cytoplasm. From Weibel (52), used with permission.**

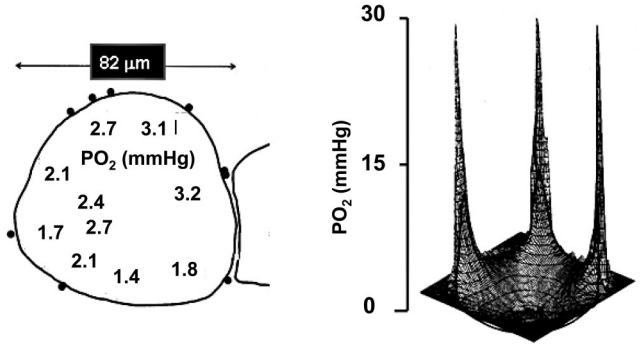


**FIGURE 2—Measurements of intramyocyte $PO_2$ during maximal exercise in the dog gracilis muscle. *Left panel*: $PO_2$ at discrete locations within the myocyte transverse plane. Solid circles at periphery designate capillaries with $PO_2$ as high as 80–90 mm Hg. *Right panel*: three-dimensional reconstruction of the $O_2$ partial pressure ($PO_2mv$) profile within the muscle capillary and the contracting myocyte ($PO_2intra$, redrawn from (15)). Note the principal $PO_2$ fall occurs in close proximity (within 0.5–2 µm) of the capillary, and that the $PO_2intra$ profile is remarkably flat without substantial $PO_2$ gradients. This suggests that even relatively large intracellular $O_2$ diffusion distances to the mitochondria, if they exist, are of little consequence.**

Thews (14) and Federspiel and Popel (11) as well as the demonstrated dependence of tissue $O_2$ diffusing capacity on capillary RBC density in frog skin (28)); and B) the intramyocyte distance for $O_2$ diffusion is immaterial for mitochondrial $O_2$ delivery with there being little opportunity for anoxic loci in healthy muscle (15).

**Site of $O_2$ offloading.** Under certain conditions, for example, in resting muscle of deeply anesthetized rodents, there is evidence that the capillaries may not constitute the sole or indeed the primary site of diffusive $O_2$ delivery. Specifically, Swain and Pittman (46) demonstrated that about two thirds of the arteriolar-venular $O_2$ loss occurred in the arterioles rather than the capillaries. Whereas this phenomenon is more likely to occur in very low flow conditions such as those present in noncontracting muscle in individuals suffering from hypotension, heart failure, or diabetes, its importance in contracting muscle remains to be determined.

## PROFILE OF CAPILLARY RBC DYNAMICS AT EXERCISE ONSET IN HEALTH

At the onset of exercise, measurements of cardiac output or blood flow ($\dot{Q}$) across the exercising limbs or muscle ($\dot{Q}m$) reveal that $\dot{Q}O_2m$ ($\dot{Q}m$ * arterial $O_2$ content) increases extremely quickly. In fact, in almost all instances $\dot{Q}m$ dynamics are appreciably faster than $\dot{V}O_2m$ dynamics (7,13,24,45,49). Although this observation suggests that $\dot{Q}O_2m$ dynamics *per se* are probably not limiting $\dot{V}O_2m$ kinetics, without knowing the spatial and temporal distribution of the increased $\dot{Q}O_2m$ within muscle, one cannot be certain that the actively contracting myocytes that have increased their $\dot{V}O_2$ requirement, have access to that $O_2$. To address this issue, Kindig and colleagues (24) used an optically gated intravital microscopy method to analyze capillary hemodynamics and RBC distribution patterns at the onset of electrically induced muscle contractions (1 Hz). The rat spinotrapezius was selected for its superb optical properties and its mixed fiber composition and oxidative capacity, which are similar to human locomotory muscles (rat (5); human (27)). As evident in Figure 3, capillary RBC velocity and flux (synonymous with $\dot{Q}m$) increased without discernible delay (i.e., <500 ms) within the first contraction–relaxation cycle (1 s) and achieved an apparent steady state within 30–45 s. Moreover, there appears to be a biphasic pattern in the RBC flux profile that coheres both with bulk $\dot{Q}m$ measurements and also with the temporal sequence of putative mediators for the exercise hyperemia (6,24,47,48). Specifically, an essentially instantaneous increase in $\dot{Q}m$ (muscle pump or rapid vasodilation of unknown origin) occurs, and is followed by a less rapid further rise of $\dot{Q}m$ to the steady state (nitric oxide, propagated

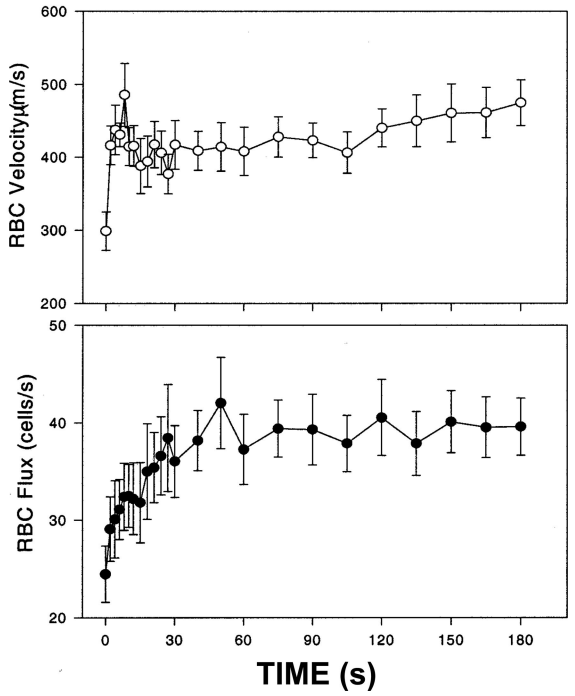


**FIGURE 3—Capillary red blood cell (RBC) velocity (*upper panel*) and flux (*lower panel*) increase within the first contraction cycle at the start of muscle contractions (time 0) in the rat spinotrapezius (electrical stimulation at 1 Hz). From Kindig et al. (24), used with permission.**

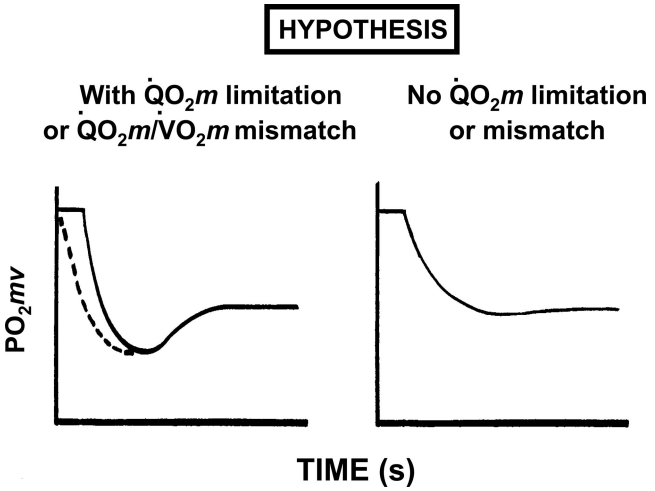


**FIGURE 5—Schematic showing hypothetical microvascular $PO_2$ ($PO_2mv$) profiles at the onset of contractions if oxygen delivery ($\dot{Q}O_2m$) is limited or there is pronounced $\dot{Q}O_2m/\dot{V}O_2m$ mismatch (*left panel*) or alternatively without $\dot{Q}O_2m$ constraint (*right panel*). See text for additional details.**

vasodilation, vasodilatory metabolites, etc.). What these measurements could not evaluate was whether, in this preparation, these $\dot{Q}m$ (and thus $\dot{Q}O_2m$) dynamics were indeed faster than those for $\dot{V}O_2m$.

## MUSCLE MICROVASCULAR $PO_2$ AND $O_2$ UTILIZATION/EXCHANGE AT EXERCISE ONSET

**Muscle microvascular pressure of oxygen, $PO_2$ ($PO_2mv$).** One technique that can measure the instantaneous relationship between $\dot{Q}O_2m$ and $\dot{V}O_2m$ is phosphorescence quenching, which was developed initially for providing rapid, high-fidelity measurements of $PO_2$ in biologic samples (42). Selection of an oxyphor (porphyrin compound that signals the oxygen-dependent quenching of phosphorescence) that can be restricted to the intravascular space enables $PO_2mv$ measurements to be made at frequent intervals without the necessity for compromising muscle vascular function (33,36). Thus, $PO_2mv$ evaluates $\dot{Q}O_2m$-to-$\dot{V}O_2m$ matching as well as measuring the $O_2$ pressure head that drives blood–myocyte $O_2$ diffusion according to Fick's law:

$$\dot{V}O_2m = DO_2m(PO_2mv - PO_2intra) \quad [1]$$

where $DO_2m$ is the muscle effective diffusing capacity and $PO_2mv$ and $PO_2intra$ are the $PO_2$'s within the microvasculature and myocyte, respectively (Fig. 4). Moreover, as contracting $PO_2intra$ is very close to zero (15), $PO_2mv$ represents the majority of the mean $PO_2$ diffusion gradient. Using this technique, Behnke et al. (4) tested the hypothesis that the capillary $\dot{Q}O_2m$ kinetics would be sufficiently rapid

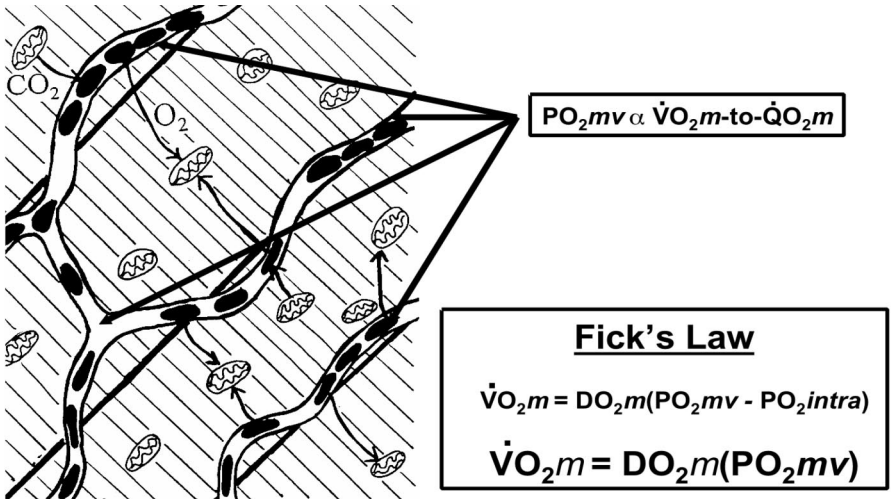


**FIGURE 4—Schematic illustration of Fick's law applied to blood–myocyte $O_2$ exchange within the microcirculation of skeletal muscle. Note: intramyocyte $PO_2$ ($PO_2intra$) approaches "zero" (1–3 mm Hg, see Fig. 2) during exercise, and thus the predominant portion of the $O_2$ gradient that drives blood–myocyte transfer is microvascular $PO_2$ ($PO_2mv$). Therefore, the $PO_2intra$ term can be discarded in the $\dot{V}O_2m$ calculation with only a modest margin of error. See text for additional details.**

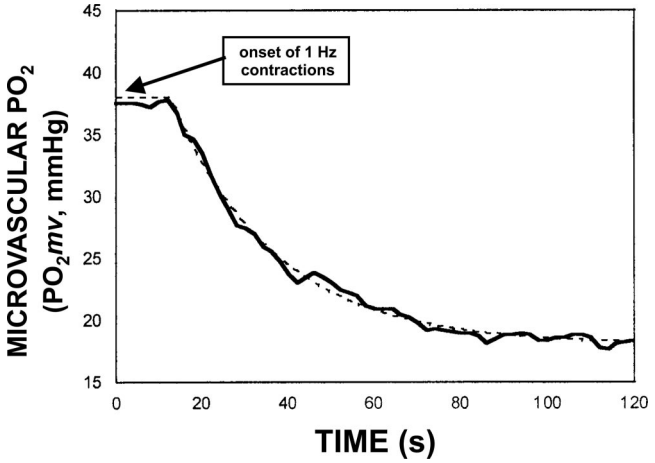


**FIGURE 6—Profile of microvascular $PO_2$ ($PO_2mv$) of the rat spinotrapezius muscle in response to contractions. Time 0 is the onset of contractions. Solid line is data gathered at 2-s intervals. *Dashed line* shows model (time delay + monoexponential) fit to the data. The constancy of $PO_2mv$ for the initial 10–20 s demonstrates that $\dot{Q}O_2m$ and $\dot{V}O_2m$ are increasing in proportion to one another. Redrawn from Behnke et al. (4).**

such that the $PO_2mv$ profile at exercise onset would not evidence an $O_2$ limitation (Fig. 5). These investigators considered that a $PO_2mv$ response that fell immediately and precipitously to values below those present in the steady state, would be indicative of a $\dot{Q}O_2m$ (and therefore an $O_2$) limitation (Fig. 5, left panel). As demonstrated in Figure 6, at the onset of contractions, $PO_2mv$ remained constant for 10–20 s before falling exponentially to the steady state. Behnke et al. (4) interpreted this profile to mean that at exercise onset the increases in $\dot{Q}O_2m$ and $\dot{V}O_2m$ were closely matched (i.e., $PO_2mv$ was unchanged for the initial 10–20 s). Subsequently, $\dot{V}O_2m$ increased at a greater rate than $\dot{Q}O_2m$, thereby driving $PO_2mv$ down to the steady-state value. There was absolutely no evidence of $PO_2mv$ falling below steady-state values as would be the expected consequence of $\dot{Q}O_2m$ being limited (relative to $\dot{V}O_2m$) across the transient (Fig. 5, left panel).

**Muscle $O_2$ utilization ($\dot{V}O_2m$) at exercise onset.** One particularly exciting opportunity arising from these investigations by Behnke et al. (4) and Kindig et al. (24) was the ability to calculate $\dot{V}O_2m$ at the site of $O_2$ transfer within the microcirculation. This is an important and contentious issue, in part, because the work of Grassi et al. (13) suggested that $\dot{V}O_2m$ increases only after a delay of several seconds from the onset of contractions. However, the concentrations of phosphate-linked controllers of mitochondrial $\dot{V}O_2$ change within the first contraction(s) (40,41,54). If there really is a mitochondrial quiescent period in the presence of intracellular perturbations thought crucial to increase mitochondrial ATP production (and therefore $\dot{V}O_2m$), current theories of metabolic control (1,31) would have to be drastically revised.

Assuming that $PO_2mv$ is qualitatively analogous to venous $PO_2$, Behnke et al. (3) combined these $PO_2mv$ measurements with capillary RBC flux at exercise onset to resolve an essentially instantaneous $\dot{V}O_2m$ (Fig. 7).

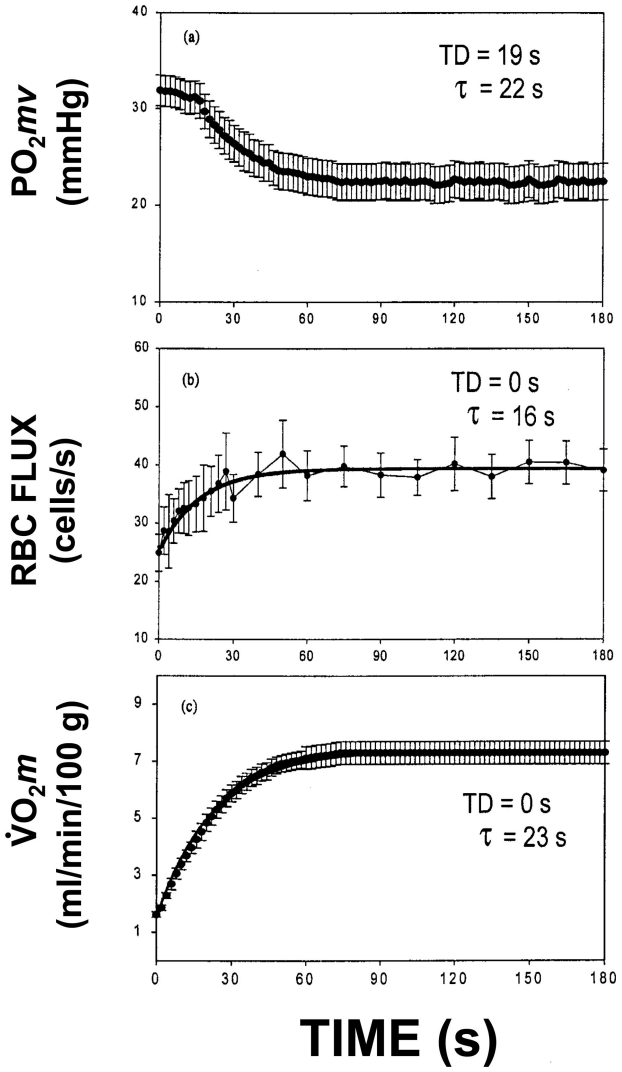


**FIGURE 7—Combining red blood cell (RBC) flux (*middle panel*) from Figure 3 and microvascular $PO_2$ ($PO_2mv$; *top panel*) from Figure 6, Behnke et al. (4) resolved the time course of microvascular (i.e., muscle) $O_2$ uptake ($\dot{V}O_2m$) in the rat spinotrapezius muscle at the onset of contractions (from time 0; *bottom panel*). Notice the absence of any detectable delay in the $\dot{V}O_2m$ response. Redrawn from Behnke et al. (3).**

Because this $\dot{V}O_2m$ is determined at the level of the microcirculation and the time resolution of the microcirculation hemodynamics measurement is <500 ms and that of $PO_2mv$ no greater than 2 s, confounding effects of microvascular RBC heterogeneities, shunts, and transit times to the site of measurement are avoided. As demonstrated in Figure 7, $\dot{V}O_2m$ increases without apparent delay from exercise onset. This conclusion arises also from the recent experiments of Kindig et al. (20) in the amphibian myocyte and Grassi et al. (12) in the dog gastrocnemius–plantaris complex. However, one point of contention here is that some of the single myocyte studies do show evidence of a delay in the fall of intramyocyte $PO_2$ at the onset of contractions, and this apparent discrepancy remains to be fully resolved (see the companion paper by Walsh et al. in this symposium's proceedings).

## EFFECTS OF DISEASE ON MICROVASCULAR FUNCTION AND $O_2$ EXCHANGE

Physiologists and clinicians who have examined exercise energetics in heart failure and diabetic populations are aware that these individuals experience extremely slow pulmonary $\dot{V}O_2$ kinetics at exercise onset (17,51). One consequence of this sluggish $\dot{V}O_2$ response is an enlarged $O_2$ deficit (53) that exacerbates the fall in creatine phosphate and other intracellular perturbations (e.g., $\Delta ADP_{free}$, $\Delta Cr$, $\Delta Pi$, $\uparrow H^+$). Thus at any given exercise intensity, glycogenolysis is stimulated to a greater extent in such patients than in their healthy counterparts, and exercise tolerance is compromised. This is particularly tragic for patients suffering from heart failure or diabetes because exercise has great therapeutic benefits that will not be realized if the patient cannot, or through discomfort will not, be physically active.

**Capillary RBC dynamics.** Figure 8 compares the profile of capillary RBC dynamics in skeletal muscle in chronic heart failure (CHF) to those observed previously in healthy muscle (37). In these animals, heart failure was induced by surgical ligation of the left coronary artery. The resultant myocardial infarction increased left ventricular end-diastolic pressure to approximately 11 mm Hg (i.e., moderate CHF), and was estimated to have destroyed approximately 30% of the left ventricular wall. In resting muscle, the percentage of flowing capillaries was reduced from 80–90% to 50–60% (21) and those capillaries that did not support RBC flux at rest did not start flowing during contractions (37). Notice that the almost instantaneous increase in RBC flux found in healthy skeletal muscle at the onset of contractions is completely absent in CHF (Fig. 8). Interestingly, within those capillaries that supported a continuous RBC flux, the Hct was not different from that found in healthy controls so that the RBC–capillary endothelium surface "contact" was reduced in approximate proportion to the reduction in flowing capillaries.

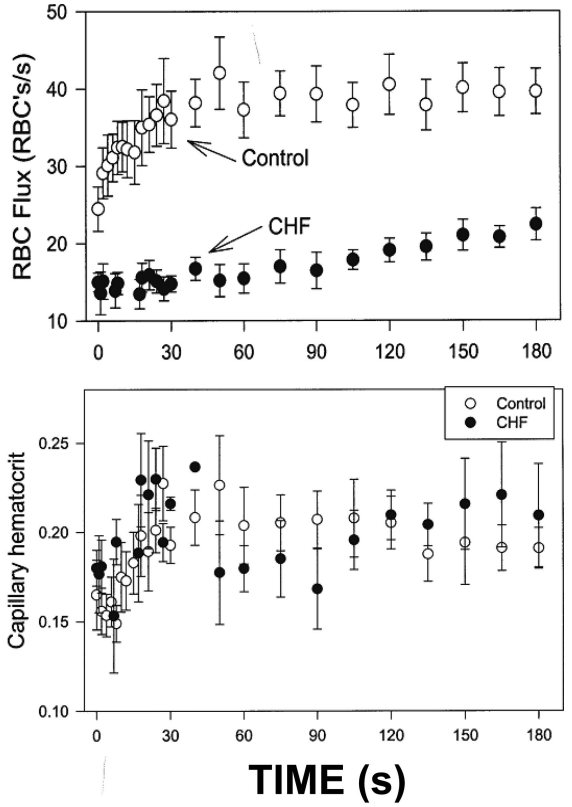


**FIGURE 8—Capillary red blood cell (RBC) flux (*upper panel*) and Hct (*lower panel*) at the onset of contractions (1 Hz initiated at time 0) in the rat spinotrapezius of control (*hollow symbols*) and chronic heart failure (CHF; *solid symbols*) animals. Notice that the immediate increase in RBC flux is not evident in CHF animals. From Richardson et al. (37), with permission.**

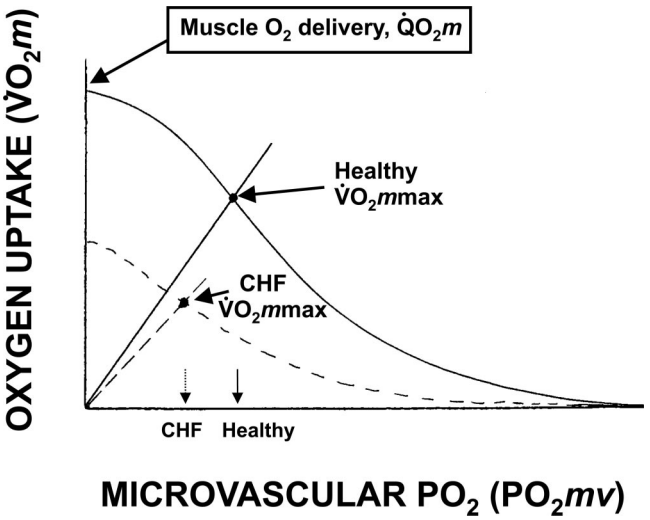


**FIGURE 9—Schematic demonstrating the determination of maximal muscle $O_2$ uptake ($\dot{V}O_2m$max) by muscle conductive ($\dot{Q}O_2m$) and diffusive ($DO_2m$) movement of $O_2$ by the cardiovascular and muscle microcirculatory systems (modeled after the "Wagner" analysis (39,50)). *Curved line* denotes mass balance according to the Fick principle ($\dot{V}O_2m = \dot{Q}m(Co_2a\text{-}Co_2mv)$ where $\dot{Q}m$ is muscle blood flow and $Co_2a$ and $Co_2mv$ are the arterial and microvascular $O_2$ concentrations, respectively), and the straight line from the origin (of slope $DO_2m$, effective diffusing capacity) represents Fick's law of diffusion. Thus, $\dot{V}O_2m = DO_2m\ (PO_2mv - PO_2intra)$. $PO_2mv$ and $PO_2intra$ are the mean $O_2$ partial pressures in the microvascular and intramyocyte compartments, respectively. $\dot{V}O_2m$max occurs at the intersection of the two lines. For the purposes of this illustration, $Co_2mv$ is considered analogous to venous $PO_2$. Note that CHF (*dashed line*) lowers $\dot{V}O_2m$max by a combination of reduced $O_2$ delivery ($\dot{Q}O_2m$) and $DO_2m$, despite $PO_2mv$ falling to lower levels in CHF than healthy controls (*solid lines*) as designated by the arrowheads on the abscissa.**

In CHF patients during submaximal exercise, the venous effluent from exercising muscles or limbs usually contains less $O_2$ than that of healthy controls (18). For many years, this led scientists and clinicians to the presumption that the ability to extract $O_2$, that is, microcirculatory function, was not impaired in these patients. However, it is evident that if $\dot{Q}m$ is low and the percentage of capillaries supporting RBC flux is reduced, there must be impaired conductive and diffusive $O_2$ delivery. Figure 9 uses the elegant analysis developed by Wagner and colleagues (39,50) to demonstrate how a pathologically low muscle $O_2$ diffusing capacity ($DO_2m$, given by the slope of the straight line projecting from the origin of Fig. 9), can coexist with reduced microvascular $O_2$ content in CHF. A major challenge facing scientists today is resolving the mechanistic bases for these

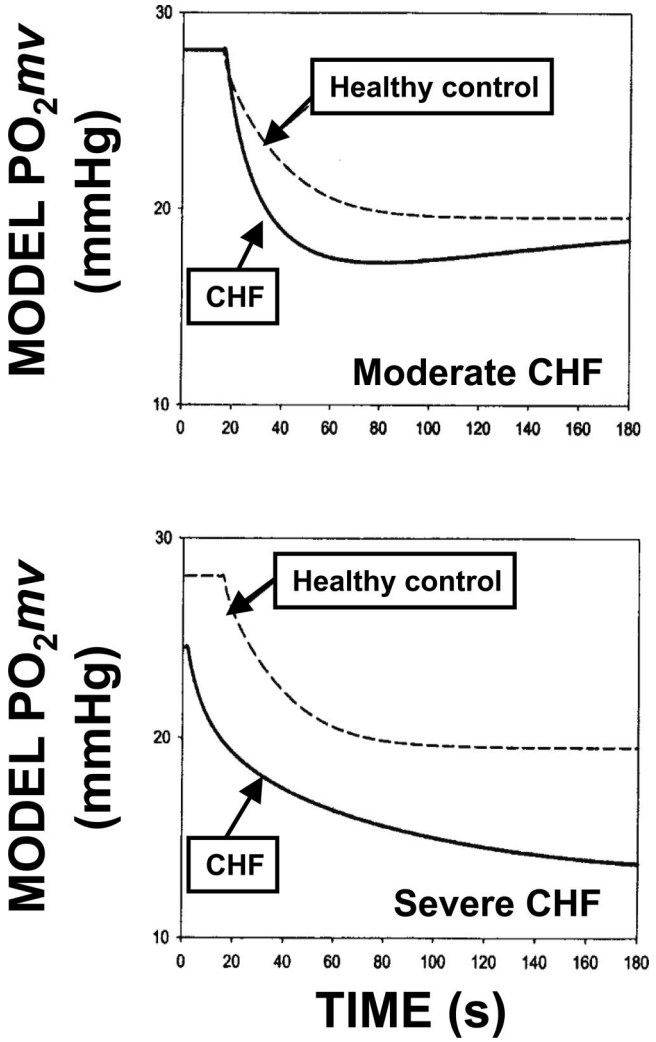


**FIGURE 10—Effect of moderate (*upper panel*) and severe (*lower panel*) chronic heart failure (CHF) on the microvascular $PO_2$ ($PO_2mv$) profile at the onset of contractions (time 0) in rat spinotrapezius muscles. Profiles are also given for healthy control (*dashed curves*) and CHF (*solid curves*) rats. Left ventricular end-diastolic pressures in the control, moderate CHF, and severe CHF were 3, 9, and 27 mm Hg, respectively (all $P < 0.05$). Note the substantial lowering of $PO_2mv$ across the transient in both CHF populations. Also note that in the severe CHF condition $PO_2mv$ remains substantially below control even in the "steady state," whereas for moderate CHF $PO_2mv$ in the steady state is not different from healthy control. Data from Diederich et al. (9).**

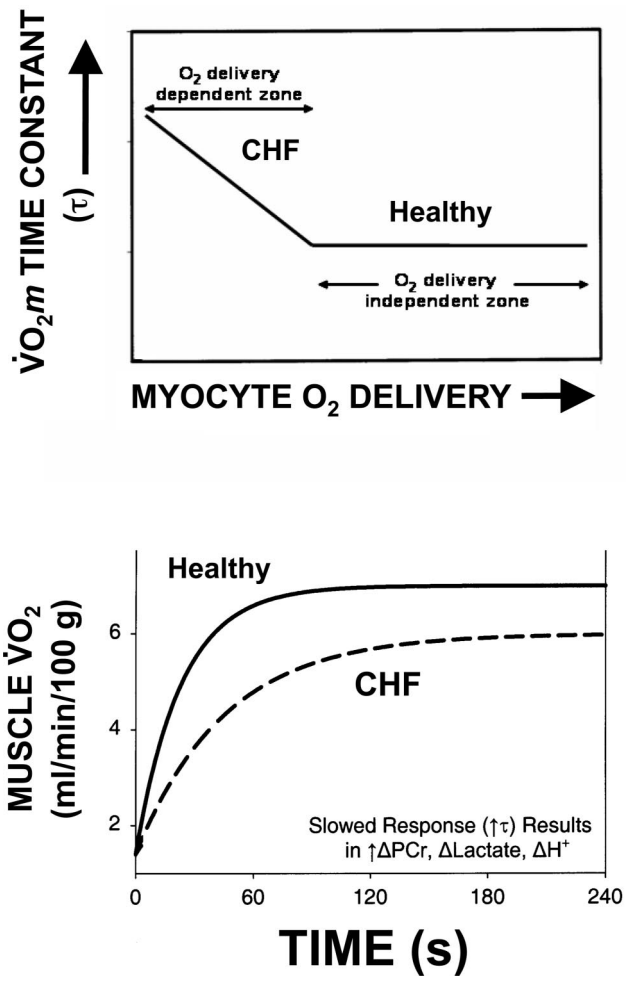


**FIGURE 11—*Upper panel:* Theoretical construct that explains the effect of altered muscle (myocyte) $O_2$ delivery on $\dot{V}O_2m$ kinetics. Within healthy muscle, $\dot{V}O_2m$ kinetics are independent of $O_2$ delivery (*right side of graph*). However, chronic heart failure (CHF) reduces both conductive and diffusive $O_2$ transport such that $\dot{V}O_2m$ kinetics (denoted by the time constant, $\tau$) become slowed (*left side of graph*). *Lower panel* depicts these slowed $\dot{V}O_2m$ kinetics present in CHF. Note the substantial increase in the $O_2$ deficit that is approximated as that area below a horizontal line projected from the asymptote (of the healthy response) back to the abscissa.**

impairments in muscle $O_2$ conductive and diffusive $O_2$ delivery and developing strategies for combating them. A detailed analysis of the key relevant derangements present in heart failure is beyond the scope of this review. However, it is worth listing some of the pathological sequelae that may impact mitochondrial $O_2$ delivery in heart failure (17): reduced bulk $\dot{Q}m$ (conductive $O_2$ delivery) (mechanisms: ↓cardiac output, ↑vessel stiffness, ↑venous congestion, ↑sympathetic tone, ↓ endothelial nitric oxide synthase, ↑circulating angiotensin II), reduced $O_2$ diffusive delivery (mechanisms: ↓proportion of capillaries supporting RBC flux, ↓total RBCs adjacent to contracting muscle fibers, $\dot{Q}O_2$-to-$\dot{V}O_2$ mismatch).

**Muscle microvascular $PO_2$ ($PO_2mv$).** In healthy muscle, we explored the hypothesis posed above that, if muscle $O_2$ delivery was indeed limiting $\dot{V}O_2m$ kinetics, $PO_2mv$ would be expected to fall immediately and precipitously at the onset of contractions (Fig. 5, lefthand side). Further, the likelihood was recognized that $PO_2mv$ would fall transiently below steady-state levels before the increase of $\dot{Q}O_2m$ to levels appropriate to sustain the increased metabolic rate (i.e., $\dot{V}O_2m$). Whereas a $\dot{Q}O_2m$ limitation was not found to be present at exercise onset in healthy muscle, we hypothesized that the plethora of pathologically induced impediments to muscle $O_2$ conduction and diffusion listed above would likely change the site of $\dot{V}O_2m$ kinetics limitation. This hypothesis was addressed in experimental animals following induction of moderate CHF in which muscle oxidative enzyme activities (e.g., citrate synthase) are preserved and severe CHF where they are not (9). This latter distinction is important where the balance between $\dot{Q}O_2m$ and $\dot{V}O_2m$ is being evaluated. Specifically, if $\dot{Q}O_2m$ dynamics are slowed in the absence of altered $\dot{V}O_2m$ kinetics

(moderate CHF), one of the $PO_2mv$ profiles shown in the lefthand side of Figure 5 is expected. However, if both $\dot{Q}O_2m$ and $\dot{V}O_2m$ are slowed (severe CHF), the $PO_2mv$ profile may simply demonstrate slow kinetics that resolve to very low $PO_2mv$ values (9). Figure 10 demonstrates the results of these experiments and provides evidence that heart failure results in a lowered microvascular $O_2$ pressure head (i.e., $PO_2mv$) across the transition to contractions that is subsequently resolved (i.e., $PO_2mv$ increases to steady-state contracting values not different from control) in CHF of a moderate but not severe nature. In both situations, however, $\dot{V}O_2m$ kinetics are expected to be slowed and the $O_2$ deficit increased because of the reduction in $PO_2mv$ across the transition to contractions in accordance with Fick's law (Fig. 11). Collectively, these results support the notion that $\dot{Q}O_2$ kinetics are not limiting $\dot{V}O_2$ kinetics in healthy muscle but may do so in diseases such as heart failure where $\dot{Q}O_2$ kinetics are so slow that $PO_2mv$ is reduced below that found in healthy skeletal muscle.

## CONCLUSIONS

Resolution of $O_2$ exchange at the muscle microvascular level is a challenging undertaking that, at present, necessitates use of selective animal models and muscles. By their very nature, these experiments must be conducted using electrically induced muscle contractions in anesthetized animals. Notwithstanding these considerations, combination of intravital microscopy and phosphorescence quenching techniques have opened a unique and informative window into vascular function and muscle energetics during contractions. In healthy muscle, capillary RBC flux and $\dot{Q}O_2m$ increase within the first contraction cycle, and this is matched by an essentially immediate and proportional increase in $\dot{V}O_2m$ such that $PO_2mv$ (and thus the driving pressure for blood–myocyte $O_2$ diffusion) is sustained across the first few seconds of the transition. Subsequently, $\dot{V}O_2m$ increases at a greater rate than $\dot{Q}O_2m$, and $PO_2mv$ falls exponentially to the steady-state level. In diseases such as chronic heart failure, $PO_2mv$ falls rapidly below healthy control values indicative of $\dot{Q}O_2$-to-$\dot{V}O_2m$ mismatching. According to Fick's law, this is expected to reduce blood–myocyte $O_2$ transfer and slow $\dot{V}O_2m$ kinetics. One consequence of slowed $\dot{V}O_2m$ (and thus pulmonary $\dot{V}O_2$) kinetics is the generation of an increased $O_2$ deficit and a greater degree of intracellular perturbation that accelerates the fatigue process. Animal models of heart failure and other diseases present the invaluable opportunity to investigate the mechanistic bases for such muscle dysfunction at a level not possible in humans and without the confounding effects of altered activity patterns and therapeutic treatments.

We are grateful to Drs. Timothy I. Musch, William L. Sexton, Paul McDonough, Casey A. Kindig, and Mrs. K. Sue Hageman, without whose expertise the experiments cited in this review would not have been possible. In particular, Dr. Casey A. Kindig (to whom this symposium was dedicated) was an absolutely superb young investigator who died tragically on April 23, 2004. He was posthumously awarded the ACSM 2004 New Investigator Award at the national meeting in Indianapolis. These investigations were funded, in part, by grants from the National Institutes of Health HL-50306, HL-69739, and AG-19228 and a Grant-in-Aid from the American Heart Association, Heartland Affiliate.

## REFERENCES

1. Balaban, R. S. Regulation of oxidative phosphorylation in the mammalian cell. *Am. J. Physiol.* 258:C377–C389, 1990.
2. Barstow, T. J., N. Lamarra, and B. J. Whipp. Modulation of muscle and pulmonary $O_2$ uptakes by circulatory dynamics during exercise. *J. Appl. Physiol.* 68:979–989, 1990.
3. Behnke, B. J., T. J. Barstow, C. A. Kindig, P. Mcdonough, T. I. Musch, and D. C. Poole. Dynamics of oxygen uptake following exercise onset in rat skeletal muscle. *Respir. Physiol. Neurobiol.* 133:229–239, 2002.
4. Behnke, B. J., C. A. Kindig, T. I. Musch, S. Koga, and D. C. Poole. Dynamics of microvascular oxygen pressure across the rest-exercise transition in rat skeletal muscle. *Respir. Physiol.* 126:53–63, 2001.
5. Behnke, B. J., C. A. Kindig, P. Mcdonough, D. C. Poole, and W. L. Sexton. Dynamics of microvascular oxygen pressure during rest-contraction transition in skeletal muscle of diabetic rats. *Am. J. Physiol. Heart Circ. Physiol.* 283:H926–H932, 2002.
6. Clifford, P. S., and Y. Hellsten. Vasodilatory mechanisms in contracting skeletal muscle. *J. Appl. Physiol.* 97:393–403, 2004.
7. Delp, M. D. Control of skeletal muscle perfusion at the onset of dynamic exercise. *Med. Sci. Sports Exerc.* 31:1011–1018, 1999.
8. Desjardins, C., and B. R. Duling. Microvessel hematocrit: measurement and implications for capillary oxygen transport. *Am. J. Physiol.* 252:H494–H503, 1987.
9. Diederich, E. R., B. J. Behnke, P. Mcdonough, et al. Dynamics of microvascular oxygen partial pressure in contracting skeletal muscle of rats with chronic heart failure. *Cardiovasc. Res.* 56:479–486, 2002.
10. Ellis, C. G., R. F. Potter, and A. C. Groom. The Krogh cylinder geometry is not appropriate for modelling $O_2$ transport in contracted skeletal muscle. *Adv. Exp. Med. Biol.* 159:253–268, 1983.
11. Federspiel, W. J., and A. S. Popel. A theoretical analysis of the effect of the particulate nature of blood on oxygen release in capillaries. *Microvasc. Res.* 32:164–189, 1986.
12. Grassi, B., M. C. Hogan, P. L. Greenhaff, et al. Oxygen uptake on-kinetics in dog gastrocnemius in situ following activation of pyruvate dehydrogenase by dichloroacetate. *J. Physiol* . 538:195–207, 2002.
13. Grassi, B., D. C. Poole, R. S. Richardson, D. R. Knight, B. K. Erickson, and P. D. Wagner. Muscle $O_2$ uptake kinetics in humans: implications for metabolic control. *J. Appl. Physiol.* 80: 988–998, 1996.
14. Groebe, K., and G. Thews. Calculated intra- and extracellular $PO_2$ gradients in heavily working red muscle. *Am. J. Physiol.* 259: H84–H92, 1990.
15. Honig, C. R., T. E. J. Gayeski, and K. Groebe. Myoglobin and oxygen gradients. In: Crystal, R.G., J.B. West, E.R. Weibel, and P.J. Barnes (eds) *The Lung: Scientific Foundations.* New York: Raven Press, pp. 1925-1933, 1997.
16. Ishikawa, H., H. Sawada, and E. Yamada. Surface and internal morphology of skeletal muscle. In: Peachy, L. D., R. H. Adrian, and S. R. Geiger (Eds.). *Handbook of Physiology.* Section 10: Skeletal Muscle, Bethesda, MD: American Physiological Society, pp. 555-631, 1983.
17. Jones, A. M., and D. C. Poole. *Oxygen Uptake Kinetics in Sport, Exercise and Medicine.* Routledge, London, 2005, pp. 353–372.
18. Katz, S. D., C. Maskin, G. Jondeau, T. Cocke, R. Berkowitz, and T. Lejemtel. Near-maximal fractional oxygen extraction by active skeletal muscle in patients with chronic heart failure. *J. Appl. Physiol.* 88:2138–2142, 2000.
19. Kayar, S. R., and N. Banchero. Sequential perfusion of skeletal muscle capillaries. *Microvasc. Res.* 30:298–305, 1985.

20. KINDIG, C. A., R. A. HOWLETT, and M. C. HOGAN. Effect of extracellular $PO_2$ on the fall in intracellular $PO_2$ in contracting single myocytes. *J. Appl. Physiol.* 94:1964–1970, 2003.
21. KINDIG, C. A., T. I. MUSCH, R. J. BASARABA, and D. C. POOLE. Impaired capillary hemodynamics in skeletal muscle of rats in chronic heart failure. *J. Appl. Physiol.* 87:652–660, 1999.
22. KINDIG, C. A., and D. C. POOLE. A comparison of the microcirculation in the rat spinotrapezius and diaphragm muscles. *Microvasc. Res.* 55:249–259, 1998.
23. KINDIG, C. A., and D. C. POOLE. Sarcomere length-induced alterations of capillary hemodynamics in rat spinotrapezius muscle: vasoactive vs passive control. *Microvasc. Res.* 61:64–74, 2001.
24. KINDIG, C. A., T. E. RICHARDSON, and D. C. POOLE. Skeletal muscle capillary hemodynamics from rest to contractions: implications for oxygen transfer. *J. Appl. Physiol.* 92:2513–2520, 2002.
25. KLITZMAN, B., and B. R. DULING. Microvascular hematocrit and red cell flow in resting and contracting striated muscle. *Am. J. Physiol.* 237:H481–490, 1979.
26. KROGH, A. The number and distribution of capillaries in muscles with calculation of the oxygen pressure head necessary for supplying the tissues. *J. Physiol. (Lond.)* 52:409–415, 1919.
27. LEEK, B. T., S. R. MUNDALIAR, R. HENRY, O. MATHIEU-COSTELLO, and R. S. RICHARDSON. Effect of acute exercise on citrate synthase activity in untrained and trained human skeletal muscle. *Am. J. Physiol. Regul. Integr. Comp. Physiol.* 280:R441–7, 2001.
28. MALVIN, G. M., and S. C. WOOD. Effects of capillary red cell density on gas conductance of frog skin. *J. Appl. Physiol.* 73:224–33, 1992.
29. MATHIEU-COSTELLO, O., C. G. ELLIS, R. F. POTTER, I. C. MACDONALD, and A. C. GROOM. Muscle capillary-to-fiber perimeter ratio: morphometry. *Am. J. Physiol* . 261:H1617–H1625, 1991.
30. MCDONOUGH, P., B. J. BEHNKE, T. I. MUSCH, and D. C. POOLE. Effects of chronic heart failure in rats on the recovery of microvascular $PO_2$ after contractions in muscles of opposing fibre type. *Exp. Physiol.* 89:473–485, 2004.
31. MEYER, R. A, and J. M. FOLEY. Cellular processes integrating the metabolic response to exercise. In: *Handbook of Physiology. Exercise: Regulation and Integration of Multiple Systems.* Bethesda, MD: American Physiological Society, sect. 12, pp. 841-869, 1996.
32. MOLE, P. A., Y. CHUNG, T. K. TRAN, N. SAILASUTA, R. HURD, and T. JUE. Myoglobin desaturation with exercise intensity in human gastrocnemius muscle. *Am. J. Physiol. Regul. Integr. Comp. Physiol.* 277: R173–R180, 1999.
33. POOLE, D. C., B. J. BEHNKE, P. MCDONOUGH, R. M. MCALLISTER, and D. F. WILSON. Measurement of muscle microvascular oxygen pressures: compartmentalization of phosphorescent probe. *Microcirc.* 11:317–326, 2004.
34. POOLE, D. C., T. I. MUSCH, and C. A. KINDIG. In vivo microvascular structural and functional consequences of muscle length changes. *Am. J. Physiol* . 272:H2107–H2114, 1997.
35. POOLE, D. C., and O. MATHIEU-COSTELLO. Capillary and fiber geometry in rat diaphragm perfusion fixed in situ at different sarcomere lengths. *J. Appl. Physiol.* 73:151–159, 1992.
36. POOLE, D. C., P. D. WAGNER, and D. F. WILSON. Diaphragm microvascular plasma $PO_2$ measured in vivo. *J. Appl. Physiol.* 79:2050–2057, 1995.
37. RICHARDSON, T. E., C. A. KINDIG, T. I. MUSCH, and D. C. POOLE. Effects of chronic heart failure on skeletal muscle capillary hemodynamics at rest and during contractions. *J. Appl. Physiol.* 95:1055–1062, 2003.
38. RICHARDSON, R. S., E. A. NOYSZEWSKI, K. F. KENDRICK, J. S. LEIGH, and P. D. WAGNER. Myoglobin $O_2$ desaturation during exercise. Evidence of limited $O_2$ transport. *J. Clin. Invest.* 96:1916–1926, 1995.
39. ROCA, J., A. G. AGUSTI, A. ALONSO, et al. Effects of training on muscle $O_2$ transport at $\dot{V}O_2$max. *J. Appl. Physiol.* 73:1067–1076, 1992.
40. ROSSITER, H. B., S. A. WARD, V. L. DOYLE, F. A. HOWE, J. R. GRIFFITHS, and B. J. WHIPP. Inferences from pulmonary $O_2$ uptake with respect to intramuscular [phosphocreatine] kinetics during moderate exercise in humans. *J. Physiol.* 518:921–932, 1999.
41. ROSSITER, H. B., S. A. WARD, J. M. KOWALCHUK, F. A. HOWE, J. R. GRIFFITHS, and B. J. WHIPP. Effects of prior exercise on oxygen uptake and phosphocreatine kinetics during high-intensity knee-extension exercise in humans. *J. Physiol.* 537:291–303, 2001.
42. RUMSEY, W. L, J. M. VANDERKOOI, and D. F. WILSON. Imaging of phosphorescence: a novel method for measuring oxygen distribution in perfused tissue. *Science* 241:1649–1651, 1988.
43. RUSSELL, J. A., C. A. KINDIG, B. J. BEHNKE, D. C. POOLE, and T. I. MUSCH. Effects of aging on capillary geometry and hemodynamics in rat spinotrapezius muscle. *Am. J. Physiol. Heart Circ. Physiol.* 285:H251–H258, 2003.
44. SARELIUS, I. H., and B. R. DULING. Direct measurement of microvessel hematocrit, red cell flux, velocity, and transit time. *Am. J. Physiol.* 243:H1018–H1026, 1982.
45. SHOEMAKER, J. K., and R. L. HUGHSON. Adaptation of blood flow during the rest to work transition in humans. *Med. Sci. Sports Exerc.* 31:1019–1026, 1999.
46. SWAIN, D. P., and R. N. PITTMAN. Oxygen exchange in the microcirculation of hamster retractor muscle. *Am. J. Physiol.* 256:H247–55, 1989.
47. THOMAS, G. D., and S. S. SEGAL. Neural control of muscle blood flow during exercise. *J. Appl. Physiol.* 97:731–738, 2004.
48. TSCHAKOVSKY, M. E., and D. D. SHERIFF. Immediate exercise hyperemia: contributions of the muscle pump vs. rapid vasodilation. *J. Appl. Physiol.* 97:739–747, 2004.
49. TSCHAKOVSKY, M. E., J. K. SHOEMAKER, and R. L. HUGHSON. Vasodilation and muscle pump contribution to immediate exercise hyperemia. *Am. J. Physiol* . 271:H1697–H1701, 1996.
50. WAGNER, P. D., J. ROCA, M. C. HOGAN, D. C. POOLE, D. E. BEBOUT, and P. HAAB. Experimental support for the theory of diffusion limitation of maximum oxygen uptake. *Adv. Exp. Med. Biol.* 277:825-833, 1990.
51. WASSERMAN, K., J. E. HANSEN, D. S. SUE, B. J. WHIPP, and R. CASABURI. *Principles of Exercise Testing and Interpretation.* Lea and Febiger, London, 1994.
52. WEIBEL, E. R. *The Pathway for Oxygen: Structure and Function in the Mammalian Respiratory System*, Harvard University press, London, pp. 399-404, 1984.
53. WHIPP, B. J., and K. WASSERMAN. Oxygen uptake kinetics for various intensities of constant-load work. *J. Appl. Physiol.* 33: 351–356, 1972.
54. YOSHIDA, T., and H. WATARI. 31P-nuclear magnetic resonance spectroscopy study of the time course of energy metabolism during exercise and recovery. *Eur. J. Appl. Physiol. Occup. Physiol.* 66:494–499, 1993.